

# THE ON-ORBIT PERFORMANCE OF THE CALIOP LIDAR ON CALIPSO

David Winker<sup>(1)</sup>, William Hunt<sup>(2)</sup>, Carl Weimer<sup>(3)</sup>

<sup>(1)</sup> NASA, MS 475, NASA Langley Research Center, Hampton, VA 23681 (USA),  
E-mail: [david.m.winker@nasa.gov](mailto:david.m.winker@nasa.gov)

<sup>(2)</sup> Science Systems and Applications, Inc, MS 475, NASA Langley Research Center, Hampton, VA 23681  
(USA), E-mail: [william.h.hunt@nasa.gov](mailto:william.h.hunt@nasa.gov)

<sup>(3)</sup> Ball Aerospace & Technologies Corp, 1600 Commerce Street, Boulder, CO 80301 (USA)  
E-mail: [cweimer@ball.com](mailto:cweimer@ball.com)

## ABSTRACT

CALIPSO is a joint NASA – CNES satellite currently in its third year of operation in low earth orbit. The satellite is making optical measurements of the Earth's atmosphere to help quantify the impact of aerosols and clouds on the Earth's radiation budget. To do this, it carries three instruments: CALIOP, a two-wavelength polarization-sensitive elastic backscatter lidar; the IIR a three band thermal imaging radiometer; and the WFC a visible single-band imager. CALIOP utilizes a Nd:YAG laser which incorporates a harmonic crystal to provide laser light at both 1064 nm and 532 nm. This beam is expanded and transmitted into the atmosphere at near nadir. The laser light scattered from clouds and aerosols back to the satellite, along with any solar background light, is collected by a one meter diameter beryllium telescope. The captured light is separated into its two wavelengths and optically filtered. The 1064 nm component is detected with an avalanche photodiode, while the 532 nm component is further resolved into two linear polarization components which are then detected by matching photomultiplier tubes. This presentation will describe the lidar and give examples of its on-orbit performance.

## 1. INTRODUCTION

CALIPSO (Cloud-Aerosol Lidar and Infrared Pathfinder Satellite Observation) is the product of collaboration between NASA and the French space agency (CNES). The CALIPSO payload combines an active lidar instrument with passive infrared and visible imagers [1]. Ball Aerospace and Technology Corporation (BATC) was the prime NASA contractor for the payload. CNES provided the PROTEUS spacecraft, built by Alcatel, and the Imaging Infrared Radiometer (IIR), developed by SODERN.

CALIPSO was launched on 28 April 2006 for a nominal three year mission, with the possibility of extension beyond that time. Its objective is to probe the vertical structure and properties of clouds and aerosols [2]. The satellite orbits in close formation with Aqua, CloudSat, Parosol and Aura as part of the Afternoon Constellation (A-Train) of Earth-observing satellites [3], in a sun-synchronous orbit at 705 km altitude with an ascending node equator crossing time of 13:30 local solar time. The orbit inclination of 98° provides coverage between 82°N and 82°S. The lidar pointing direction, initially 0.3° off nadir, was changed to 3.0° off nadir in November, 2007.

The primary instrument on CALIPSO, and the subject of this paper, is Cloud Aerosol Lidar with Orthogonal Polarization (CALIOP), a three-channel elastic-backscatter lidar. CALIOP has been acquiring backscatter data both day and night almost continuously since routine operations began on 13 June 2006

A brief description of the lidar will be given, followed by a discussion of its on-orbit performance.

## 2. LIDAR DESCRIPTION

### 2.1 Overview

CALIOP makes range-resolved measurements of elastic backscatter at 532 nm and 1064 nm, with the two wavelength measurements providing information about particle sizes. Backscatter measurements are made for two orthogonal polarizations at 532 nm, thereby providing information about the shapes of the backscattering particles. A dynamic range of more than six orders of magnitude provides linear measurements of all targets of interest, from molecules above 30 km to PBL water clouds at 1 km. A large amount of on-board data processing provides increased automation, reduced downlink data rate, and enhanced monitoring capabilities through the extraction of

selected science data for inclusion in the Health and Status data.

A block diagram of the transmitter and receiver is shown in Fig. 1.

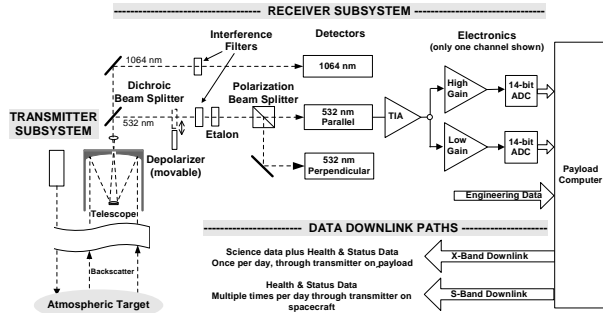


Fig. 1. Simplified block diagram of CALIOP

## 2.2 Transmitter

The transmitter is a Q-switched diode pumped Nd:YAG laser that is frequency-doubled to produce simultaneous pulses at 1064 nm and 532 nm. A beam expander reduces the output beam divergence, and a beam steering mechanism provides the capability to optimize the boresight alignment between the laser and the receiver. A second identical laser, as yet unused on orbit, provides redundancy in case of a problem with the primary laser.

Key transmitter parameters are given in Table 1.

Table 1 CALIOP Transmitter Specifications

Wavelengths	532 nm and 1064 nm
Pulse energy at each wavelength (nominal)	110 mJ
Repetition rate	20.16 Hz
Ground spot spacing	335 m
Polarization purity at 532 nm	> 99%
Beam divergence at each wavelength (nominal)	110 microrad
Line width at 532 nm	28 pm

## 2.3 Receiver

The backscattered light is collected by a one-meter diameter all-beryllium telescope. A dichroic beam

splitter separates the two wavelengths, and a polarization beam splitter separates the 532 nm beam into components parallel to and perpendicular to the laser polarization. Each of the three beam components goes to its own detector. The 532 channel detectors are photomultipliers (PMTs) and the 1064 channel detector is an avalanche photodiode (APD).

After going through a transimpedance amplifier (TIA), the output of each of the three detectors is split and sent in parallel to two amplifiers with different gains, each of which is followed by a 14-bit digitizer (designated the high gain digitizer and the low gain digitizer for simplicity). The two digitizer outputs are later merged during on-board processing, resulting in an effective dynamic range of more than 21 bits.

Solar background rejection is provided by a narrowband etalon in combination with a dielectric interference filter in the 532-nm channels, and an interference filter alone in the 1064 nm channel. A pseudo-depolarizer can be moved into the 532 nm beam upon command for measurement of the relative sensitivities of the two polarization channels.

Key receiver specifications are given in Table 2.

TABLE 2 CALIOP Receiver Specifications

Telescope diameter	1 meter
Field of View	130 microrad
Optical Filter Bandwidth (532 nm)	35 pm
Optical Filter Bandwidth (1064 nm)	400 pm
Digitizer sample rate	10 MHz
Vertical sample spacing	15 m
Electronic bandwidth	2.0 MHz
Vertical resolution as determined by bandwidth	30 m
Digitizer resolution	14 bits
Maximum dynamic range (merged)	2.5E6 (>21 bits)

## 2.4 On-board processing

The lidar is autonomously reconfigured for night or day, based the Earth-Sun-Satellite angle, which is computed using data from the on-board GPS receiver. In order to make most effective use of the digitizer dynamic range as the background noise changes, the gains and offsets need to be different for night and day.

The data acquisition timing is adjusted on every shot, based upon the range to sea level as computed from GPS data.

The mean signals from background light and detector dark noise are subtracted electronically prior to digitization.

The d.c. offset signals to the digitizers are subtracted digitally.

Signals from the high and low gain digitizers on each channel are merged.

Backscatter signals are averaged horizontally and vertically, with the amount of averaging depending upon the altitude. This averaging, when combined with other on-board processing, reduces the downlink data rate by more than an order of magnitude, without the loss of essential information.

Background noise, mean backscatter signals, and other quantities are computed from the science data and placed in the Health and Status data, allowing for monitoring of the lidar performance from status data alone, without the need to go to the much more cumbersome science data.

### 3. LIDAR PERFORMANCE

The following sections will discuss the performance of the instrument only. Performance of the data processing algorithms will not be discussed except for cases where the algorithm performance is directly related to the instrument performance. Similarly, independent measurements to validate algorithm performance will not be discussed.

#### 3.1 Performance overview

In most respects the performance of CALIOP has been excellent, allowing the production of high quality science data products. The amount of adjustment that has been required to maintain the performance over more than two years has been minimal, consisting mostly of boresight alignments.

Areas where the performance has been less than ideal are mostly related to thermally-induced misalignment during the sunlit portions of orbits and radiation effects on the laser and detectors, primarily in the South Atlantic Anomaly (SAA).

#### 3.2 Laser energy

The primary laser has shown very little degradation in energy, continuing to produce more than 94% of its initial energy at both wavelengths, with no adjustments

(Fig. 2). The backup laser has not yet been fired on orbit.

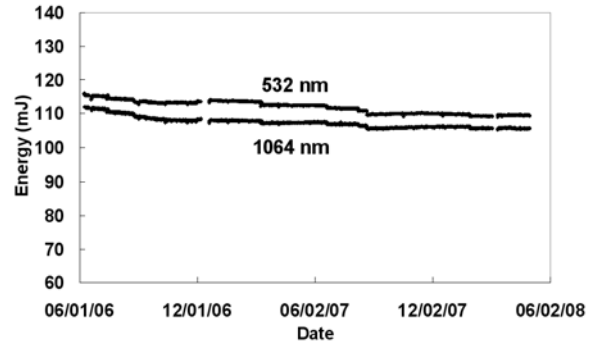


Fig. 2 Laser Energy Trend

#### 3.3 Laser pressure

Each laser is housed in its own sealed canister filled with dry air at standard atmospheric pressure. A slow loss of pressure was noted in the primary laser before launch, and that trend has continued (Fig. 3). The backup laser has maintained its pressure well.

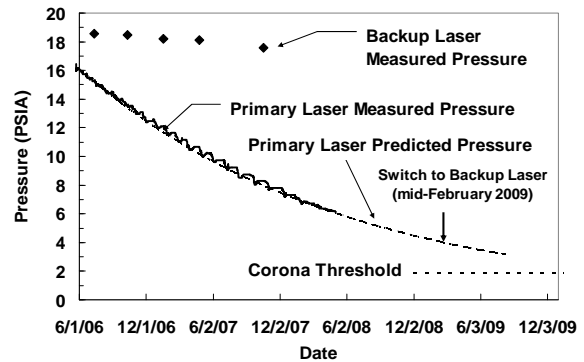


Fig. 3 Canister Pressure Trends

As of September 2008 the primary laser pressure is approximately 5 PSIA. At this level, low pressure is causing no problems, but there is a potential for a corona discharge due to the high voltage within the canister if the laser operation is continued to below about 1.9 PSIA. A switch to the backup laser is currently planned for mid February 2009, well before the pressure reaches the corona threshold.

#### 3.4 Signal-To-Noise Ratio (SNR)

The single-shot SNR of CALIOP is extremely low because of its high altitude and modest power-aperture product. However, the SNR can be improved by horizontal and vertical averaging, with the amount of allowable averaging limited by the spatial scale of the target of interest. During the design phase SNR requirements were defined for various targets and

background lighting conditions for each channel, with specified amounts of averaging. On-orbit SNR measurements confirm that all the requirements are being met, with a significant amount of margin in most cases.

The most critical SNR requirement is that for the 532 parallel channel at night when measuring molecular backscatter from 30 km, since this measurement is the basis for the calibration of all channels, day and night. The measured SNR for this case soon after launch was about 83, well above the required value of 50. All subsequent measurements have given values well above 90% of the initial value (Fig. 4). The lowest value was observed when both the boresight alignment and the etalon tuning had drifted somewhat from their optimum settings. There was a significant improvement after these drifts were corrected. The SNR of the 532 perpendicular channel very nearly duplicates that of the parallel channel when they experience the same backscatter signal levels.

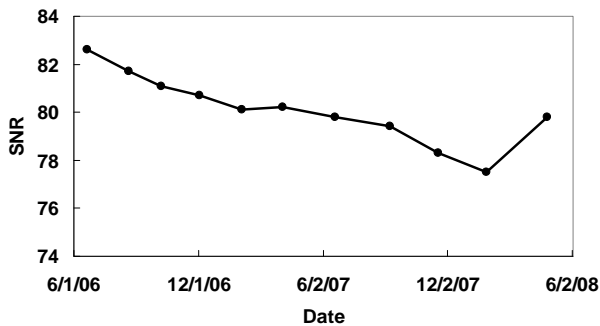


Fig. 4 SNR trend for the 532 parallel channel at night

The nighttime SNR of the 1064 channel is interesting because it shows the effects of radiation damage to the APD (discussed later). Fig. 5 shows that the nighttime SNR for this channel under specified conditions has decreased by more than 35% since its initial on-orbit measurement, reflecting the increased APD dark noise. Such a decrease was expected, though its magnitude could not be readily predicted with the available pre-launch information. There is no nighttime requirement on this channel, but the daytime SNR remains more than a factor of 3 above the requirement.

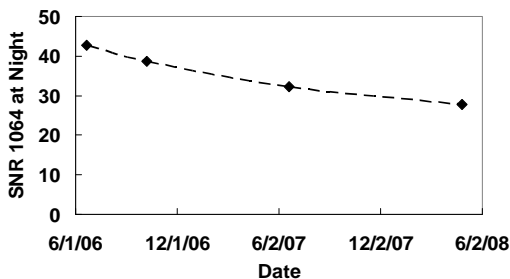


Fig. 5 SNR trend for the 1064 Channel at Night

### 3.5 Overall Sensitivity

The 532 parallel channel is calibrated at multiple locations throughout each nighttime orbit segment by comparing the measured backscatter signal with the expected signal from 30-34 km altitude, where the expected signal for a given time and geographic location can be derived from molecular and ozone number densities provided by NASA's Global Modeling and Assimilation Office (GMAO). The calibration coefficient is a good indicator of the overall detection sensitivity of the lidar, since it defines the relationship between the backscatter coefficient of the target and the signal measured by the lidar. Fig. 6 shows how the calibration coefficient has changed over time. In late 2007 it had dropped to about 87% of its initial value, but it recovered to more than 95% of its initial value after a boresight alignment and retuning of the etalon. As expected, this behavior closely parallels the SNR trend shown in Fig. 4.

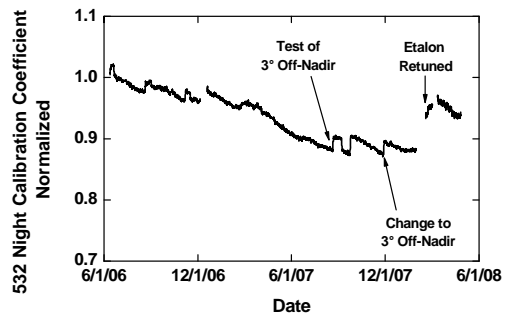


Fig. 6 Calibration coefficient trend for the 532 parallel channel at night

### 3.6 Boresight Alignment Stability

The lidar transmitter has a beam steering mechanism that allows the pointing direction to be adjusted along two orthogonal axes. At relatively infrequent intervals, a boresight alignment is carried out by offsetting the laser pointing direction by fixed amounts in four different directions and making high altitude backscatter signal measurements at each position. Based upon the relative signals at the four points, a new optimum pointing direction is computed and implemented. Boresight alignments cannot be performed in daylight because the SNR is too low to make the required signal measurements.

Fig. 7 shows that the laser pointing direction after alignment has shown a slow and fairly systematic drift over the course of the mission, with the current position being about 40 microradians away from the initial aligned position. This drift is believed to be due

to distortion of the laser canister as its pressure has decreased.

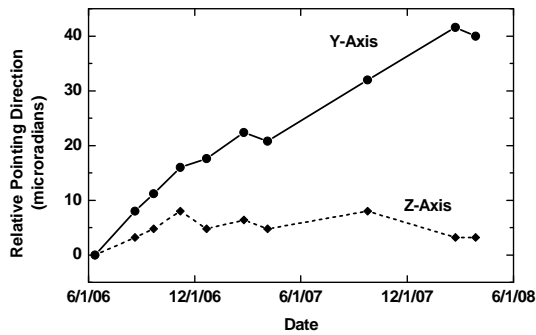


Fig. 7 History of the aligned pointing direction

While the aligned positions in Fig. 7 indicate relatively stable alignment, these data are only indicative of the 532 channel alignment during the dark portion of each orbit.. There is indirect evidence that the alignment is less stable when the satellite is in sunlight, as will be discussed in the following paragraphs.

When the 532 channel nighttime calibration coefficient is plotted as a function of latitude, the coefficient is relatively constant through the dark portion of the orbit, indicating stable alignment, but it starts to drop off once the satellite gets into sunlight, possibly indicating a thermally induced boresight alignment.

Once the sunlight reaches the clouds and surface below the satellite, the SNR becomes too low to continue the calibration measurements, and also too low to carry out boresight alignments. Thus the daylight alignment accuracy must be inferred from other measurements such as the scattering ratio. The scattering ratio is the ratio of the measured backscatter signal to the expected signal from a purely molecular atmosphere, and it should have a value near unity at all latitudes for appropriate cloud-free profiles. Daytime scattering ratios can be computed for appropriate targets by selecting only cloud-free profiles and performing large amounts of averaging. When computed in such a manner using the measured nighttime calibration coefficient, the scattering ratio consistently drops below unity during the daylight portion of each orbit, with the amount of drop depending upon both the latitude and the time of the year. Fig. 8 shows the scattering ratio averaged over the entire month of January 2007, computed using the nighttime calibration coefficient, and plotted as function of the time after the start of the daylight portion of the orbit. The scattering ratio is below unity for the entire center portion of the orbit, dropping to about 0.7 at the lowest point, indicating that the calibration coefficient at that point in the orbit has changed by about 30% relative to its

nighttime value. Curves for other months show similar behavior, with the minimum value varying according to the time of year. This behavior is taken to indicate a thermally-induced boresight alignment shift during the sunlit orbit segment, with the amount of shift being a function of the solar beta angle.

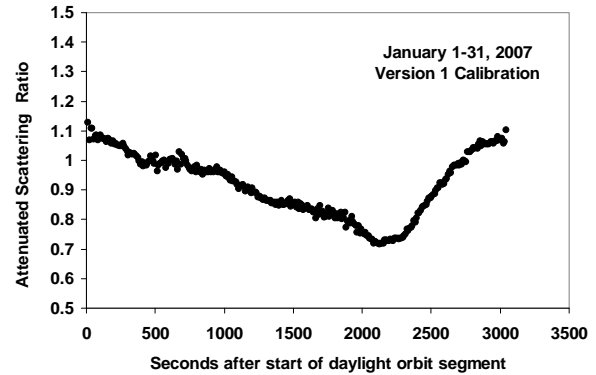


Fig. 8 Scattering ratio during daylight orbit segments in January 2007

This effect has been taken into account in the most recent data release (Version 2.01), in which the daytime calibration algorithm in the level 1 processing software has been modified to make use of empirical data such as is shown in Fig. 8.

The effect of alignment shifts on the 1064 channel backscatter signal is more difficult to analyze. Any alignment shift should be common to both the 532 channel and the 1064 channel, but the backscatter signals will be affected differently because the laser outputs at the two wavelengths have different spatial beam profiles and different effective divergences. There is also the possibility that the beams at the two wavelengths are not perfectly co-aligned.

Some insight can be obtained by looking at the backscatter signals from fairly intense high altitude cirrus clouds. Such clouds are assumed to be “white”, so that the ratio of the backscatter signals at the two wavelengths is expected to be constant, independent of latitude and time of day. Fig. 9 is a scatter plot of several days of raw data from such clouds for two different times of year. The normalized 1064/532 raw signal ratio is plotted as a function of latitude, with dark data shown as blue crosses and sunlit data shown as red circles. The arrows indicate the direction of satellite motion for each. These plots show that the channel ratio when the satellite is in sunlight differs from that when it is in the dark, with amount of difference being a function of both latitude and time of year. This has much similarity to the 532 channel daytime behavior shown in Fig. 8, again indicating a boresight misalignment when the satellite is in the sun.

The variation in the ratio of the two wavelengths shows how the misalignment affects the signals from the two wavelengths differently.

An unexpected aspect of Fig. 9 is that the channel ratio is a function of latitude for both night and day, at all times of year. Possible explanations for this behavior are being investigated.

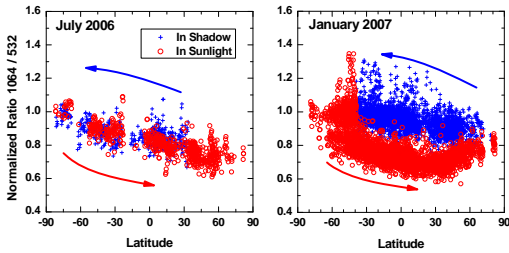


Fig. 9 Normalized channel ratio (1064 / 532) for signals from intense cirrus clouds

### 3.7 Polarization Gain Ratio

The relative sensitivity of the two 532 nm channels is measured occasionally by inserting a pseudo-depolarizer into the beam so that equal amounts of light fall upon both detectors. The polarization gain ratio (PGR) is the ratio of the signals from the two channels during this operation. The PGR is used for calibrating the 532 perpendicular channel signal. Fig. 10 shows that the PGR increased slowly during the first year, and has been quite stable since that time.

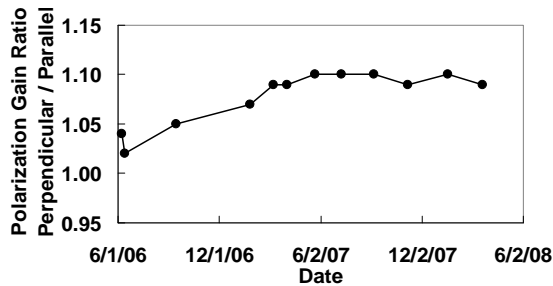


Fig. 10 Polarization Gain Ratio trend

### 3.8 Polarization cross talk

The ratio of the calibrated 532 perpendicular channel signal to the calibrated 532 parallel channel signal is the volume linear depolarization ratio (or depolarization ratio, for short). CALIOP is designed to measure the depolarization ratio of clouds and aerosols, but it is not expected to be sensitive enough to make accurate measurements of the depolarization ratio of clear air (estimated to be approximately 0.37% at the bandwidth of the CALIOP optical filter [4]).

Nevertheless, it is informative to look at the values obtained from clear air measurements because those values are useful for putting an upper limit on the amount of crosstalk between the two polarization channels. Early in the mission the clear air depolarization ratio was measured to be 0.6%, but later it made an abrupt jump to 0.9%, and since then it has made several abrupt jumps both up and down (Fig. 11). Even with the higher values, the total crosstalk is still less than the 1% design objective. The abrupt jumps occur after changes in the thermal conditions, and are believed to be associated with unrelieved stress on the etalon after thermal changes.

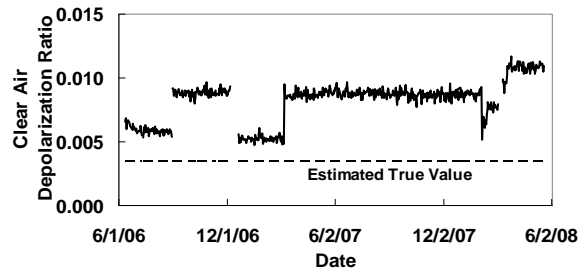


Fig. 11 Clear air depolarization ratio measurement trend

### 3.9 Etalon Tuning

The passband of the 532 channel etalon was chosen to be about the same as the line width of the laser, so as to reduce the solar background as much as possible without excessive attenuation of the laser energy. With the filter passband so close to the laser line width, the two center wavelengths must be well matched in order to optimize the laser throughput. The center wavelength of the etalon is controlled by adjusting its temperature, but there is no active feedback mechanism to keep the etalon center wavelength matched to that of the laser. An etalon temperature scan in February 2008 showed that the center wavelengths between the laser and the etalon had become mismatched by about 7 pm since the start of the mission. An adjustment of the etalon temperature resulted in about a 6% increase in the backscatter signal.

### 3.10 Radiation Effects

At its 705 km altitude, CALIPSO is exposed to cosmic radiation at all times, with the flux becoming particularly intense while passing through the South Atlantic Anomaly (SAA). This results in several undesirable effects on the lidar, as described in the following paragraphs.

When exposed to cosmic radiation, the photomultipliers can produce current pulses that are as much as two orders of magnitude larger than pulses due to single photoelectrons, resulting in increased noise levels and possible biases in the measured backscatter signals. Fig. 12 is a color-coded plot of the photomultiplier RMS dark noise as a function of geographic location for all night orbits over a sixteen day repeat cycle in the fall of 2006.

The dark noise in the middle of the SAA, which stands out as a bright region just to the left of center, is more than 30 times higher than it is outside the SAA. Radiation bands near the poles are visible as lighter blue curved lines. The straight lighter lines across the plot at  $\pm 65^\circ$  are due to scattered light when the satellite goes into and out of sunlight.

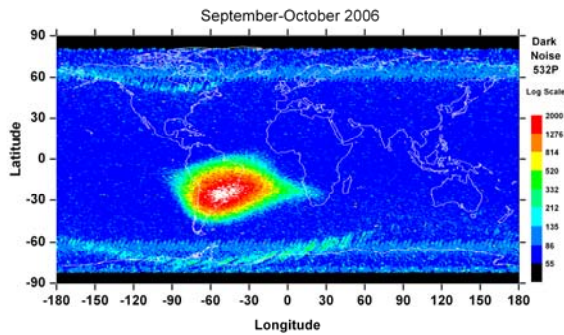


Fig. 12 Dark noise map for the 532 parallel channel

Special provisions have been made in the data processing to minimize the effects of these noise pulses, especially in the SAA.

Previous studies [5] have shown that APDs in a space environment experience an increase in bulk dark current that is proportional to the cumulative radiation exposure, so that the dark noise can be expected to increase in a manner that is proportional to the square root of the cumulative dosage. Fig. 13 shows that the CALIOP 1064 channel APD has shown a dark noise increase consistent with that expectation. Most of the SNR decrease shown in Fig. 5 is a direct result of this dark noise increase.

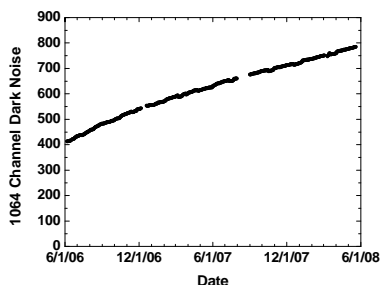


Fig. 13 1064 channel dark noise trend

CALIOP has experienced two additional effects that appear to be a result of radiation exposure, though the root causes have not yet been determined.

The laser occasionally “misfires”, producing isolated shots whose energy is lower than normal, sometimes as low as zero. These shots occur most frequently in the SAA, indicating that they are radiation related. The frequency of such shots is currently quite low, so that their impact on science data quality is negligible. However, their frequency is steadily increasing, and changes are being made in the data processing software to minimize their effects in the future, should their frequency continue to rise.

Finally, there have been several occasions in recent months when the laser went into a fault condition, resulting in the payload transitioning to Safe mode. All of these faults have occurred when the satellite was in the SAA, and all indications are that they were the result of single event upsets caused by radiation. Flight software changes are being made to minimize the impact of such events in the future.

#### 4. REFERENCES

1. Winker, D. M., Pelon, J. and McCormick, M. P., The CALIPSO mission: Spaceborne lidar for observation of aerosols and clouds, *Proc. SPIE*, 4893, 1-11, 2003
2. Winker, D. M., Hunt, W. H. and McGill, M. J.: Initial performance assessment of CALIOP, *Geophys. Res. Lett.*, 34, L19803, doi:10.1029/2007GL030135, 2007
3. Stephens, G. L., et. al, The CloudSat Mission and the A-Train: A New Dimension of Space-Based Observations of Clouds and Precipitation, *Bulletin of the American Meteorological Society*, vol. 83, number 12, pp. 1771-1790, 2002
4. Cairo, F., et. al., Comparison of various linear depolarization parameters measured by lidar, *Appl. Opt.* 38, 4425-4432, 1999.
5. Sun, X., et al, Measurement of Proton Radiation Damage to Si Avalanche Photodiodes, *IEEE Transactions on Electron Devices*, vol. 44, issue 12, pp. 2160-2166, 1997